

# UCSF

## UC San Francisco Previously Published Works

### Title

Towards BirthAlert--A Clinical Device Intended for Early Preterm Birth Detection.

### Permalink

<https://escholarship.org/uc/item/99k9v6vp>

### Journal

IEEE Transactions on Biomedical Engineering, 60(12)

### Authors

Etemadi, Mozziyar

Chung, Philip

Heller, J

et al.

### Publication Date

2013-12-01

### DOI

10.1109/TBME.2013.2272601

Peer reviewed



# HHS Public Access

Author manuscript

*IEEE Trans Biomed Eng.* Author manuscript; available in PMC 2015 October 14.

Published in final edited form as:

*IEEE Trans Biomed Eng.* 2013 December ; 60(12): 3484–3493. doi:10.1109/TBME.2013.2272601.

## Towards BirthAlert—A Clinical Device Intended for Early Preterm Birth Detection

**Mozziyar Etemadi\*** [Student Member, IEEE],

Department of Bioengineering and Therapeutic Sciences, University of California, San Francisco, CA 94158 USA

**Philip Chung,**

Department of Bioengineering and Therapeutic Sciences, University of California, San Francisco, CA 94158 USA (philip.chung@ucsf.edu).

**J. Alex Heller** [Student Member, IEEE],

University of California, San Francisco, CA 94158 USA, and also with the University of California, Berkeley, CA 94720 USA (james.heller@ucsf.edu).

**Jonathan A. Liu,**

Keck School of Medicine, University of Southern California, Los Angeles, CA 90089 USA (liuja@usc.edu).

**Larry Rand,** and

Department of Obstetrics and Gynecology and Reproductive Sciences, University of California, San Francisco, CA 94143 USA (larry.rand@ucsf.edu).

**Shuvo Roy** [Member, IEEE]

Department of Bioengineering and Therapeutic Sciences, University of California, San Francisco, CA 94158 USA (shuvo.roy@ucsf.edu).

### Abstract

Preterm birth causes 1 million infant deaths worldwide every year, making it the leading cause of infant mortality. Existing diagnostic tests such as transvaginal ultrasound or fetal fibronectin either cannot determine if preterm birth will occur in the future or can only predict the occurrence once cervical shortening has begun, at which point it is too late to reverse the accelerated parturition process. Using iterative and rapid prototyping techniques, we have developed an intravaginal proof-of-concept device that measures both cervical bioimpedance and cervical fluorescence to characterize microstructural changes in a pregnant woman's cervix in hopes of detecting preterm birth before macroscopic changes manifest in the tissue. If successful, such an early alert during this “silent phase” of the preterm birth syndrome may open a new window of opportunity for interventions that may reverse and avoid preterm birth altogether.

### Keywords

Bioimpedance; bluetooth; fluorescence; physiologic sensing; sensors; spectroscopy

---

\* (Mozziyar.Etemadi@ucsf.edu).

## I. Introduction

Preterm birth contributes to 35% of the world's 3.1 million neonatal deaths each year, making it the leading cause of infant mortality [1]. Of the 15 million babies born preterm each year, almost 1 million of them die as a result of their prematurity. For infants who survive preterm birth, prospective studies have confirmed that a substantial portion of these infants experience long-term morbidity and lifelong disability [2]. This condition alone costs the United States over \$26.2 billion per year [3]. The last 30 years of preterm birth research has led to the widely accepted theory that preterm birth is a syndrome—the end result of a multitude of pathological mechanisms that may be unrelated in origin [4]–[6]. These pathological mechanisms accelerate the normal timing of parturition, leading to premature cervical softening, ripening, shortening, effacement, dilation, and finally preterm birth (see Fig. 1).

### A. Current Clinical Technologies

Current diagnostic gold standards include transvaginal ultrasound and the fetal fibronectin (fFN) immunoassay, which, respectively, use cervical length and vaginal fetal fibronectin concentration as surrogate metrics [7].

Diagnosis with transvaginal ultrasound hinges on the knowledge that a short cervix is correlated with the occurrence of preterm birth [8], [9]. Perhaps the greatest limitation to transvaginal ultrasound is that it relies on the examination of macroscopic shortening of the cervix, which generally correlates with mid- or late-stage events in the parturition process (see Fig. 1). Other limitations include data acquisition and interpretation being highly dependent on the ultrasound machine operator, with poor resolution of ultrasound images contributing to the difficulty in interpretation. Furthermore, diagnostic results are strongly dependent on patient-specific gynecologic history, gestational age at time of measurement, and can be complicated by normal biological variability [10].

The fetal fibronectin (fFN) immunoassay is an *in vitro* biochemical test that detects the presence of fetal fibronectin in the vaginal canal. Fetal fibronectin is a protein that originates within the uterus and serves to bind the fetal membranes to the uterine lining. From weeks 22 to 30 of gestation, low vaginal fFN levels indicate preterm labor will not occur in the following 7–10 days [11], [12]. While this test has a high negative predictive value (NPV = 98–99%) for predicting no labor within 7 days, it has a low positive predictive value (PPV = 14–19%) for predicting labor within 7 days [13]. Because clinicians cannot be reasonably confident that a positive-tested patient will give birth preterm, these patients can only be prescribed bed rest and watched closely. As a result, the fFN test is generally used only to monitor high risk or symptomatic pregnancies in which negative results can definitively rule out imminent preterm birth [14].

These shortcomings have led researchers to investigate diagnostic techniques that attempt to detect earlier signs of preterm birth, such as changes in the cervical microstructure during the cervical softening and ripening stages (Fig. 1).

## B. Collagen During Parturition

The cervix comprises of approximately 10% smooth muscle and 90% extracellular connective tissue, of which approximately 70–80% of the connective tissue in the cervix is collagen with the rest consisting of proteoglycans, glycosaminoglycans (GAGS), and other fibers, such as elastin [15]–[18]. During collagen fibril formation, tropocollagen is stabilized into semicrystalline collagen fibrils by covalent cross-links. One type of cross-link that is present in cervical collagen contains an aromatic pyridinoline unit. Fibrils are then bundled together into collagen fibers, with proteoglycans such as decorin helping determine size and packing of fibrils (see Fig. 2) [19].

Throughout a majority of pregnancy, cervical collagen remains in fibers, imparting a great deal of structural rigidity and mechanical stiffness to the cervix. However, during cervical softening and ripening, there is a decrease in both pyridinoline cross-link concentration and proteoglycan concentration [20]–[24]. Decrease in these collagen-organizing units at both the fiber and fibril level of collagen dramatically increases the disorganization of collagen in the cervix [25]. At the same time, the concentration of GAGS such as hyaluronan (HA) increases [26]–[28]. Hyaluronan binds water, increasing tissue hydration and filling the space created by the disorganization of extracellular matrix fibers [29]–[32]. Thus, as gestational age increases, cervical collagen crosslink concentration decreases while cervical tissue hydration increases. This inverse relationship of tissue matrix organization and hydration is largely responsible for transforming the cervix from a closed gate sealing the fetus in the uterus to an open gateway during delivery.

## C. Noninvasive Detection Methods for Cervical Microstructure Change

Two methods have gained traction in research for detecting cervical tissue microstructure changes. These are light-induced fluorescence spectroscopy (LIF) and electrical impedance spectroscopy (EIS).

LIF depends largely on the autofluorescent properties of pyridinoline collagen cross-links, which become excited by light around 370 nm and emit light around 420 nm. Prior research in rats, guinea pigs, and humans have shown strong correlations between cervical LIF measurements and cervical ripening, and a preliminary human study has shown LIF can be used to predict if a woman will deliver within 24 h [16], [33]–[36].

EIS measures change in bioelectric impedance in cervical tissue as the extracellular matrix becomes more disorganized and hydration increases. EIS involves injecting AC signals at various frequencies into cervical tissue. Tissue possesses inherent signal filtering properties because low-frequency signals tend not to penetrate cellular membranes, whereas high-frequency signals generally penetrate cellular membranes. Thus, interrogation at different frequencies result in magnitude and phase values reflective of different components within the tissue [37]. As cervical tissue becomes more disorganized and increasingly hydrated during the softening and ripening process, the tissue's electrical permittivity changes and can be observed as variations in impedance magnitude and phase [38], [39]. Human studies with tetra-polar pencil probe EIS implementations have found that an impedance measurement is indicative of labor within 24 h, but not a statistically better predictor than using the Bishop

score, which is the current clinical standard for assessing the cervix to confirm if labor [40]–[42].

#### D. Our Approach

We have developed a prototype medical device that acquires both cervical LIF and EIS measurements. This device involves a removable probe that attaches to both a cervical LIF measurement system and a cervical EIS measurement system (see Fig. 4). To our knowledge, this is the first attempt to use both techniques in parallel for detection of preterm birth. However, several differences in both approach and device design mark a departure from existing detection efforts.

Many predecessor devices have been used to predict labor or Phase III of parturition (see Fig. 1), which occurs during the last few hours of pregnancy. At this point in pregnancy there is a paucity of time for clinicians to diagnose exact cause of preterm birth, making it difficult to treat the underlying pathology; instead, the current standard of care involves administering tocolysis to try to stall the inevitable preterm birth and steroids to force rapid development of fetal lungs before the baby is born. In contrast, we have designed our device specifically with the goal of earlier detection during the cervical softening and ripening stages, which occur during Phase I and II of parturition (see Fig. 1). An early alert days or weeks ahead rather than hours would provide clinicians ample time and opportunity to conduct further diagnostic tests to pinpoint the underlying pathology and adjust patient care plans accordingly. However, the challenge is that these earlier parturition processes do not manifest macroscopically and are thus clinically silent.

By acquiring preliminary cervical LIF and EIS measurements, we aim to capture the temporal changes in these signals over gestation. We hypothesize that the trending of these signals in combination with signal fusion techniques will allow for detection earlier than using either cervical LIF or EIS alone.

## II. *In Vitro* Collagen Measurement

Collagen gels were used to model extracellular components of cervical tissue across gestation. Lyophilized type I collagen from bovine calfskin (C3511, Sigma-Aldrich, St. Louis, MO, USA) was dissolved in an acidified phosphate buffered saline (PBS) solution adjusted to pH 3.5 with 10-M acetic acid prepared in PBS. The solution was allowed to stand at room temperature for 1 day. Gelation was induced by adding 10-M NaOH (prepared in PBS) until pH 7.4 was achieved [24], [43], [44]. Serial dilution with  $1 \times$  PBS yielded samples with concentrations ranging from 1 to 50 mg/mL. Between dilutions, samples were degassed and homogenized with centrifuge and vortex mixer, respectively. Samples were then degassed in a desiccator and incubated in 96-well plates at 37 °C overnight.

Electrical impedance and fluorescence of our collagen gels were characterized using a precision impedance analyzer (Agilent Technologies 4294 A, Santa Clara, CA, USA) connected to platinum wire electrodes, and a fluorescence microplate reader (TECAN Infinite 200 Pro, Männedorf, Switzerland). Data from these instruments are shown in Fig. 3.

### III. Device Design

#### A. Intravaginal Probe

Seen in Fig. 4(a) and (b), the intravaginal probe consists of six titanium electrodes and one optical fiber port for impedance and fluorescence measurement, respectively. These sensor interfaces are embedded within implant grade medical silicone (PN40029, Applied Silicone, Santa Paula, CA, USA), which is molded into a cup-like shape designed to form-fit the human cervix. Bulk silicone was shaped and cured using a technique similar to liquid silicone injection molding. Molds for the process were designed in SolidWorks 3-D CAD software (Dassault Systems, Waltham, MA, USA) and 3-D printed via fused deposition modeling with a uPrint Plus (Stratasys, Eden Prairie, MN, USA). Three probe sizes were designed and manufactured corresponding to cup diameters of 22, 25, and 28 mm.

A custom-designed fiber optic tube in the intravaginal probe serves as a female receptacle for the fiber optic bundle attached to the fluorescence measurement system. A BK-7 window (Swiss Jewel, Philadelphia, PA, USA) seals the cervix-facing part of the tube. The internal tube geometry is designed to have a spacer that ensures consistent positioning of the fiber optic bundle when it is clamped in place with a threaded end cap.

Each electrode is wired to a modified micro USB 3.0 cable, which is connected to the impedance measurement system via female USB 3.0 receptacle. Electrodes were made from grade 2 titanium and custom designed to have circular fins on the lateral sides of the electrode to increase surface area and provide better adhesion to the silicone bulk material. Fins were treated with medical grade primer (PN40096, Applied Silicone, Santa Paula, CA, USA) and sealed using implant grade RTV silicone adhesive (PN40076, Applied Silicone, Santa Paula, CA, USA). Details of the fabrication process are described in Chung *et al.* (*in review*).

#### B. Fluorescence Measurement System

The excitation subsystem (see Fig. 4(c)) comprises of a dual LED light source (WFC-H2-0365-0385, Mightex, Ontario, Canada) with UV LEDs centered at 365 and 385 nm connected to a USB-controlled monochromator with 6-nm bandwidth resolution (SMDC1-03, Optometrics, Ayer, MA, USA) via optical fiber. Light exiting the monochromator is transmitted along the excitation fibers of the fiber optic bundle (QF600-8-VIS/NIR, Ocean Optics, Dunedin, FL, USA) and through the BK-7 window to the cervical tissue. Fluorescent light emitted from the cervical tissue is transmitted through the BK-7 window along the emission fibers of the fiber optic bundle through two long-wave pass filters with cut-on frequencies at 400 nm (FSR-GG400, Newport) and 420 nm (FSR-GG420, Newport). The resultant light signal is detected by a USB fiber optic spectrometer (USB2000, Ocean Optics). We have written custom software that controls wavelength selection of the monochromator as well as data acquisition through the spectrometer.

#### C. Impedance Measurement System

The impedance measurement system (see Fig. 4(c)) utilizes a bipolar electrode measurement design. A tunable Wien bridge oscillator was used to generate 1, 2, 5, 10, 20, and 50 kHz

sine wave signals. Three off the shelf square-wave oscillator ICs (LTC6930, Linear Technology, Milpitas, CA, USA) followed by seventh-order passive elliptical filters (Coilcraft, Cary, IL, USA) were used for generation of 1, 2, and 4 MHz sine wave signals. Frequency selection was accomplished via a signal multiplexer, which outputs the signal to an op-amp-based voltage controlled current source (VCCS). The VCCS was designed to output a  $\pm 10 \mu\text{A}$  signal and virtual ground reference, which enter multiplexers to select electrode pairs for sampling. A modified micro USB 3.0 cable is used to interface the impedance measurement system and the electrodes on the intravaginal probe. Two 9-V batteries were used to power the impedance system.

Impedance measurement was accomplished by using a gain phase detector IC (AD8302, Analog Devices, Norwood, MA, USA) with the difference between the voltage input and output from the VCCS being proportional to electrical impedance magnitude and phase. Magnitude and phase measurements were then digitized via a 24-bit ADC (LTC 2400, Linear Technology, Milpitas, CA, USA) and transmitted wirelessly via Bluetooth 2.1 (RN-42, Roving Networks, Los Gatos, CA, USA) to a computer with custom software for data acquisition. The same software also controls frequency selection and electrode selection as well as data acquisition through the fluorescence measurement system.

#### IV. Clinical Proof of Concept

Under an IRB approved study at the University of California, San Francisco Medical Center, we have collected early cervical EIS and LIF data from a high-risk pregnant woman using our prototype. During clinical examination, the subject was placed in the dorsal lithotomy position. The intravaginal probe was connected to both fluorescence measurement system and impedance measurement systems via the fiber optic port and USB connector, respectively. A Graves speculum was inserted into the vagina and the cervix was visualized. Excess cervical mucus was cleaned with a cotton-tipped swab and  $\text{dH}_2\text{O}$ . Then, a sterilized intravaginal probe was inserted with firm force applied to ensure the silicone cup wrapped around the cervix. Test measurements were taken via electrode pairs to ensure electrode contact is achieved. Then, full EIS and LIF scans were taken. Full scans were taken at two positions—"12-o-clock" and "6-o-clock". The former position indicates the BK-7 window oriented ventrally or toward the patient's navel, and the latter position indicates the BK-7 window oriented dorsally. The first time a subject was measured, the subject's cervix is fitted to one of the device sizes based on visual confirmation and test measurements. The best-fit device was then assigned to that subject for future measurements. Preliminary results from a 12-o-clock measurement from our first patient are shown in Fig. 5.

#### V. Discussion

##### A. In Vitro Experiments

*In vitro* acellular collagen gels were designed to mimic the dynamic range of the extracellular environment of cervical tissue across gestation with respect to its electrical and fluorescence properties. Gels were made chiefly to inform the overall design of our *in vivo* circuit (i.e., dynamic range), and not necessarily reproduce all aspects of cervical biology. Typically, pregnant women exhibit cervical collagen concentrations within the range of 10–

20 mg/mL of collagen depending on the extent of the cervical ripening process [23], [45]–[48]. The decrease in collagen concentration coincides with the decrease in pyridinoline crosslink concentration. As collagen concentration decreases, proteoglycan and GAG concentration have been shown to increase [23], [27]–[29], [48], [49]. Since GAGs such as hyaluronic acid bind water, increases in proteoglycans and GAGs result in increased tissue hydration. Our model approximates this effect with a lower collagen-to-PBS ratio in lower density collagen gels. The results shown in Fig. 3 show the fluorescent excitation/emission peaks for collagen lie around 370 nm/420 nm. Changes in fluorescence counts, impedance magnitude, and impedance phase are a function of collagen concentration, and the range of values is in concordance with the literature [15], [24], [33]–[35], [39], [41]–[43], [50]–[52].

A clear limitation of our model is the lack of cervical cells as well as other extracellular matrix components, such as hyaluronic acid. In cervical tissue, epithelial and stromal cells will contribute additional resistive and capacitive effects to electrical impedance measurements, but the effect of collagen concentration and tissue hydration on impedance measurements is reasonably approximated with our model. With respect to fluorescence, the lack of cells means that all fluorescence can be attributed solely to collagen.

## B. Iterative Design Methodology

We have been successful in leveraging a combination of rapid prototyping tools and bioengineering techniques to dramatically lower both cost and time necessary for the development and manufacturing of complex medical devices targeted for clinical studies. By using physiologically relevant collagen gels to approximate cervical tissue progression throughout gestation, we were able to create a bench-top model of the cervix that aided iterative development of both electrical and optical design. Use of a controlled model mimicking human-specific parameters allowed the development of a device specifically for clinical studies without requiring validation on tissue biopsies. We avoided using an animal model because anatomical differences in cervical morphology would preclude useful feedback during the iterative design process given the pressure- and position-dependent nature of electrical impedance measurements.

Having tuned a majority of design parameters in the electrical and optical subsystems, we then proceeded to validate our design in nonpregnant human subjects. At the same time, human testing allowed us to iteratively develop a mechanical design for the intravaginal probe specific to human cervixes. This approach to medical device development enabled us to begin human testing just after 4 months. Notably, all test subjects claimed little to no sensation of the device at all during placement and use, with the exception of the speculum. Iterative refinement of the intravaginal probe, electrical impedance, and fluorescence subsystems ensued for another year before we opened our clinical study to high-risk pregnant women.

Our ability to achieve short design cycles of a few months was due in part to the rapidly falling cost of electronics and growing popularity of tools such as low-cost 3-D printing. These technologies enabled us to keep a majority of the development and all of the testing in-house. Furthermore, despite low production volumes, we were able to produce these devices at a relatively low cost (see Table I).



### C. Intravaginal Probe

By using an in-house 3-D printer to create molds for the intravaginal probe and using a custom injection system similar to liquid silicone injection molding, we were able to inexpensively iterate and hone in on a suitable design for the intravaginal probe. Further details regarding this process, can be found in Chung *et al.* (*in review*).

Molds were designed to enable precise alignment of electrodes as well as the fiber optic tube. Electrodes were positioned to target stromal tissue, which is the site of extracellular matrix changes during cervical softening and ripening. The cup-like design for the tip of the intravaginal probe was a consequence of arranging electrodes on both the bottom and sides of the cup to generate spatial diversity in impedance measurements. Furthermore, whereas other researchers have used loaded-spring mechanisms in pencil-probe designs to saturate force-dependent variability in impedance measurements, we exploited the elasticity of the bulk silicone material itself via the form-fitting cup-like design to accomplish the same goal [52].

The intravaginal probe was designed with a fiber optic tube to receive a fiber optic bundle to enable reuse of the same fiber optic bundle in multiple probes that are each individually assigned to a study subject. BK-7 glass was chosen for the window because of its excellent transmission in both visible and ultraviolet wavelengths.

Because metal and silicone do not easily bond to one another, all metal components in the intravaginal probe were designed with circular fins that allow liquid silicone to seep in between the fins during the injection and curing process to better adhere metal and silicone. Posttreatment with silicone primer and RTV silicone adhesive enhanced the strength of this junction while ensuring water tightness.

The difference in sizing for the intravaginal probe tip is to account for the biological variability of human cervixes. Cup diameters of 22, 25, and 28 mm on the intravaginal probe were chosen based on trial and error from our iterative development process as well as existing data for cervical cap fitting [53]–[55].

### D. Fluorescence Measuring System

We designed our cervical LIF measurement system based on existing devices such as the SureTOUCH Collascope (Reproductive Research Technologies, Houston, TX, USA) as well as excitation and emission data from our collagen gels (see Fig 3) [15], [33]–[35], [50], [51], [56]–[59]. The Collascope uses an excitation wavelength centered at 339 nm and segments emitted wavelengths with a monochromator before detecting with a CCD spectrometer. Our device differs in that it uses a monochromator to select excitation wavelengths between 355 and 405 nm. Long-wave pass filters at 395 nm prior to the CCD spectrometer attenuates reflected excitation light from our measurement and ensures only emitted light is detected (see Fig. 4). A limitation to the current setup is the large physical size of the optical setup as well as the need for many components, although once excitation/emission peaks of interest have been selected, the optical setup can be simplified to using only LEDs and photodetectors with filter coatings built into each photodetector. Another limitation is that our range of excitation wavelengths is dictated by the narrow wavelength spread of our LED

light sources. Furthermore, use of the long-wave pass filters result in ignoring emission wavelengths below 395 nm.

We believe the limitations in wavelengths are acceptable because the main collagen peak can still be captured in the 400–450 nm range. Interpreting fluorescence of *in vivo* collagen around 420 nm is challenging due to the effects of hemoglobin absorption around this wavelength, which makes collagen appear to have two overlapping peaks centered at approximately excitation/emission 320 nm/400 nm and 370/450 nm [24]. This effect is notably absent in our collagen gel models, which exhibits emission maxima at 420 nm. Another complication in data interpretation arises from the fact that NADH from cervical cells also fluoresces at 450 nm when excited between 320 and 390 nm. Fortunately, collagen contributes approximately 70–80% to cervical tissue fluorescence, making it likely that we can capture changes in the aggregate collagen-NADH peak [24], [43], [60].

The benefits of using LED light sources include dramatic reductions in size, cost, and power consumption when compared to using other UV-generating light sources, such as xenon arc lamps. We have explored other off-the-shelf UV-light sources, including lower wavelength LEDs centered around 330–340 nm, and have found that most are not bright enough to achieve a measurable fluorescence.

## E. Electrical Impedance Measuring System

The EIS measurement system is battery powered and data are transmitted wirelessly to eliminate any physical connection to electricity mains, maximizing the safety of the device. The range of measurement frequencies was chosen to capture differences in magnitude and phase based on collagen gel impedance data (see Fig. 3). A discrete set of representative frequencies was chosen for practical reasons since scanning additional frequencies would dramatically increase the impedance scanning time due to settling time for oscillators and electrode multiplexing, making measurements impractically long. We designed the system to acquire all fluorescence and impedance data in approximately 1 min. Limitations of the current system include the lack of power optimization and the large physical size of the EIS printed circuit board, designed as such to facilitate hand soldering of the board. The impedance magnitude and phase from the EIS system are computed by converting the magnitude and phase output voltages of the AD8302 to physical magnitude and phase using a first-order conversion obtained from the manufacturer's datasheet. Notably, this approach preserves additional phase shifts imparted on the output from the circuit itself, namely, the inverting amplifier and patient protection circuitry. Future iterations of the device will calibrate out these values, however, as the device is chiefly designed to trend measurements over time, such a calibration may not be required.

The EIS measurement system uses a bipolar electrode configuration in order to perform a four-terminal sensing to acquire impedance signals. This differs from other researchers who have pursued a tetrapolar configuration, which removes contact impedance that arises from the measurement electrodes and epithelial tissue layer, but results in complex voxel-dependent sensitivity, which can be either positive or negative within a volume conductor such as tissue [37], [61]–[64]. In a bipolar configuration, contact impedance decreases

measurement accuracy, but the resultant measurement does not have a complex spatial dependency with only positive sensitivity voxels within the volume conductor.

We selected the bipolar electrode configuration to remove the possibility of decreasing measurement sensitivities, especially given the complex electrode placement around the cup-like probe tip as shown in Fig. 4. Because bipolar measurements have positive sensitivities at all voxels, we can vary electrode pair placement in  $x$ -,  $y$ -, and  $z$ -dimensions and easily compare impedance data between different electrode pairs since there is no complex sensitivity field affecting measured impedance. To our knowledge, researchers have thus far only examined cervical EIS at the distal face of the cervix and not at the lateral sides of the cervix. Our motivation for tracking both the face and lateral sides of the cervix is that impedance values may vary spatially in cervical tissue across gestation. Any force-dependencies in contact impedance are removed by the unique design of the intravaginal probe since the silicone cup-like structure fits tightly around the cervix to provide sufficient pressure on the electrodes in order to saturate force-dependency in impedance measurement.

Many existing tetrapolar impedance measurement systems are designed for use as a point-of-care device for either labor or cervical cancer detection in which a single impedance scan is used to make a diagnostic conclusion. This goal lends itself to the tetrapolar method because of the requirements for boosting measurement accuracy and removal of contact impedance contributions to attain an absolute measurement. However, we are interested in monitoring the change of cervical impedance over time as the cervical softening and ripening processes progresses. In this case, we can leverage data comparisons over time to remove static impedances in our measurement system such as the impedance of titanium electrodes. Difficult-to-control variables such as cervical mucosa can also be similarly attenuated.

## F. Human Data

Seven of 40 total pregnant subjects have been recruited to date and detailed presentation of all data will be the subject of future work. Fig. 5 depicts the preliminary data captured in a single scan on one high-risk pregnant woman at 37 gestational weeks. At this time, cervical collagen crosslinking is at a minimum and should result in minimum collagen fluorescence. Despite this, the collagen peak can still be observed at around emission wavelengths of 500 nm, indicating that our device can capture the full dynamic range of collagen fluorescence. Peaks at 400 nm are excitation light that bleeds through our 395-nm cut-on filters. The choice to allow light bleed-through is intentional to allow emission data and perhaps impedance to be normalized to the detected excitation light. Peaks at 800 nm are attributed to the second-order harmonic excitation light, which serves as another reference for normalizing collagen fluorescence.

Different electrode pair combinations provide results within the expected range. However, it is interesting to note the spatial-dependent differences in impedance signals. Differences in the detected impedance magnitude and phase of electrode pairs on the left side (A-B, B-C) and right side (D-E, E-F) of the device indicate that the cervix has shortened and effaced to the point that it is difficult for the cup-like geometry of the device to fit completely around the cervix. Visual observation of the cervix confirmed that it had indeed shortened and

approximately 2-cm-dilated at the time this measurement was taken. The increased magnitude and phase of impedance on the left side suggests that electrodes A-B and B-C may have had poor tissue contact during this measurement. However, given that the device was designed to form-fit the cervix at earlier stages of parturition to track early changes in cervical tissue, this is an acceptable limitation for our device. As we continue to examine data throughout pregnancy, we will determine whether trends in impedance can be established earlier in the parturition process.

## VI. Conclusion

We have utilized rapid prototyping and iterative techniques to develop an intravaginal device using both bioimpedance and fluorescence to characterize microstructural changes in a pregnant woman's cervix in hopes of detecting preterm birth before macroscopic changes manifest in the tissue. Data collected from a high-risk pregnant woman are promising as we continue to examine clinical study data using data trending and signal fusion techniques.

## Acknowledgment

The authors would also like to thank S. Lim for assisting in collagen gel development, J. Jambulingam for assisting in the production of devices for the clinical study, and R. Grossman-Khan and P. Ottoson for assisting in device production and coordinating all of our clinical efforts. They would also like to thank all pregnant and non-pregnant subjects for their time and feedback in developing this device.

This work was supported by the Bill and Melinda Gates Foundation, the Vodafone Americas Foundation, and the FDA under Grant 2P50FD003793.

## Biography



**Moziyar Etemadi** (S'07) received the B.S. and M.S. degrees in electrical engineering from Stanford University, Stanford, CA, USA, in 2008 and June 2009, respectively, and the Ph.D. degree in bioengineering from the University of California, San Francisco, USA/University of California, Berkeley, USA, Joint Graduate Group in Bioengineering in 2013, as part of the joint M.D./Ph.D. program.

He is currently in the Medical Scientist Training Program at the University of California, San Francisco. His current research interests include translational biomedical engineering for in-home monitoring of disease and biomedical instrumentation for fetal surgery.

Dr. Etemadi was named *Forbes Magazine's* "Top 30 Under 30" in Science in January 2012 for some of the work described in this paper. In 2011, he helped lead of a research team awarded second prize in the Vodafone Americas Wireless Innovation Challenge and the

mHealth Alliance Award. While at Stanford University in 2009, he received the Frederick E. Terman Award for Scholastic Achievement in engineering and also received the Electrical Engineering Fellowship, providing full support for his graduate studies.



**Philip Chung** received the B.S. degree in bioengineering from the University of California, Berkeley, USA, in 2010 and the M.S. degree in bioengineering jointly between the University of California, Berkeley, and University of California, San Francisco, USA, in 2011.

He is currently a Junior Specialist at the University of California, San Francisco, where he is conducting translational biomedical engineering projects in collaboration with the Departments of Surgery and Obstetrics and Gynecology.

Mr. Chung received the Berkeley Regents and Chancellors Scholars Award and Alumni Leadership Award in 2006 and 2009, respectively. In 2011, his team won the Berkeley Venture Labs Competition and was also selected as a finalist to the 2012 GSMA Mobile Health University Challenge in Cape Town, South Africa. He is a member of the Tau Beta Pi Engineering Honor Society.



**J. Alex Heller** (S'12) received the B.S. degree in mechanical engineering from the University of Southern California, Los Angeles, USA, in 2008.

He then went on to work for Northrop Grumman, Marine Systems, Sunnyvale, CA, USA. Since 2010, he has been an Engineer and Researcher at the University of California, San Francisco, for the Biomedical Microdevices Laboratory and the Pediatric Device Consortium. He is currently enrolled in the joint M.S. Bioengineering program between the University of California, Berkeley, USA, and the University of California, San Francisco. His current research is focused on medical devices, specifically, on renal replacement therapy and obstetrics-related devices.



**Jonathan A. Liu** received both the B.S. and M.S. degrees in electrical engineering from Stanford University, Stanford, CA, USA, in 2008 and 2009, respectively.

Currently, he is a first-year medical student at the Keck School of Medicine, University of Southern California in Los Angeles, CA, USA. Prior to his medical career, he was an electrical engineer in the Roy Lab, under the direction of Professor S. Roy, and in collaboration with the Pediatric Device Consortium at the University of California, San Francisco, CA, USA. His research interests include the development of low-cost medical devices, especially in the fields of surgery and pediatrics, and embedded systems.



**Larry Rand**, biography not available at the time of publication.



**Shuvo Roy** (M'96) received the B.S. degree (*magna cum laude*), with general honors for triple majors in physics, mathematics (special honors), and computer science from Mount Union College, Alliance, OH, USA, in 1992, and the M.S. degree in electrical engineering and applied physics and the Ph.D. degree in electrical engineering and computer science from Case Western Reserve University, Cleveland, OH, USA, in 1995 and 2001, respectively.

He is currently an Associate Professor in the Department of Bioengineering and Therapeutic Sciences, a joint Department of the Schools of Pharmacy and Medicine, University of California, San Francisco (UCSF), and the Director of the UCSF Biomedical Microdevices Laboratory. He holds the Harry Wm. and Diana V. Hind Distinguished Professorship in Pharmaceutical Sciences II in the UCSF School of Pharmacy. He is also a Founding

Member of the UCSF Pediatric Devices Consortium, which has a mission to accelerate the development of innovative devices for children health, and a faculty affiliate of the California Institute for Quantitative Biosciences (QB3). From 1998 to 2008, he was the Co-Director of the BioMEMS Laboratory in the Department of Biomedical Engineering, Cleveland Clinic, Cleveland, OH, USA, where he was with basic scientists, practicing clinicians, and biomedical engineers to develop microelectromechanical systems (MEMS) solutions to high-impact medical challenges. While pursuing his doctorate degree, he conducted research in the areas of design, microfabrication, packaging, and performance of MEMS for harsh environments. He also investigated microstructural characteristics and mechanical properties of MEMS materials, developed the requisite microfabrication technologies, and demonstrated operation of the first surface micromachined silicon carbide transducers at high temperatures (up to 950 °C). He has also developed miniaturized microrelays for high-performance electrical switching and ice detection sensors for aerospace applications. He joined UCSF in 2008 to continue the development of biomedical devices including wireless physiological monitoring systems and bioartificial replacement organs, and participate in the training of professional students in the School of Pharmacy as well as graduate students in the UCSF/University of California, Berkeley Joint Graduate Group in Bioengineering. He has contributed to more than 90 technical publications, coauthored three book chapters, been awarded 16 U.S. patents, and given more than 70 invited presentations.

Dr. Roy is an Associate Editor of Biomedical Microdevices and Editorial Board Member of Sensors and Materials. He is the recipient of a Top 40 under 40 Award by Crains Cleveland Business in 1999 and the Clinical Translation Award at the second Annual BioMEMS and Biomedical NanotechnologyWorld 2001 meeting. In 2003, he was selected as a recipient of the TR100, which features the worlds 100 Top Young Innovators as selected by Technology Review, the Massachusetts Institute of Technology's Magazine of Innovation. In 2004, he was presented with a NASA Group Achievement Award for his work on harsh environment MEMS. In 2005, he was named as a Whos Who in Biotechnology by Crains Cleveland Business. In 2005 and 2007, he was recognized as a Cleveland Clinic Innovator. In 2009, he was nominated for the Biotechnology Industry Organizations Biotech Humanitarian Award, which is given in recognition of an individual has used biotechnology to unlock its potential to improve the earth.

## References

1. Blencowe, H.; Cousens, S.; Chou, D.; Oestergaard, MZ.; Say, L.; Moller, A.; Kinney, M.; Lawn, J. 15 million preterm births: priorities for action based on national, regional and global estimates. In: Howson, CP.; Kinney, MV.; Lawn, JE., editors. *Born Too Soon— The Global Action Report on Preterm Birth*. World Health Organization; Geneva, Switzerland: 2012. p. 17-31.
2. Moster D, Lie RT, Markestad T. Long-term medical and social consequences of preterm birth. *New England J. Med.* Jul; 2008 359(3):262–273. [PubMed: 18635431]
3. Behrman, RE.; Butler, AS. *Preterm Birth: Causes, Consequences, and Prevention*. National Academies Press; Washington, DC, USA: 2007.
4. Gotsch F, Romero R, Erez O, Vaisbuch E, Kusanovic JP, Mazaki-Tovi S, Kim SK, Hassan S, Yeo L. The preterm parturition syndrome and its implications for understanding the biology, risk assessment, diagnosis, treatment and prevention of preterm birth. *J. Maternal-Fetal Neonatal Med.* Jan; 2009 22(Suppl. 2):5–23.

5. Goldenberg RL, Culhane JF, Iams JD, Romero R. Preterm birth 1: Epidemiology and causes of preterm birth. *Lancet*. 2008; 371:75–84. [PubMed: 18177778]
6. Romero R, Espinoza J, Kusanovic JP, Gotsch F, Hassan S, Erez O, Chaiworapongsa T, Mazor M. The preterm parturition syndrome. *BJOG: Int. J. Obstetrics Gynaecology*. Dec; 2006 113(Suppl.): 17–42.
7. Iams JD. Prediction and early detection of preterm labor. *Obstetrics Gynecol*. Feb; 2003 101(2): 402–412.
8. Iams JD. The length of the cervix and the risk of spontaneous premature delivery. *New England J. Med*. Jun; 1996 334(9):567–572. [PubMed: 8569824]
9. Owen J, Yost N, Berghella V, MacPherson C, Swain M, Dildy GA, Miodovnik M, Langer O, Sibai B. Can shortened midtrimester cervical length predict very early spontaneous preterm birth? *Amer. J. Obstetrics Gynecology*. Jul; 2004 191(1):298–303.
10. Berghella V, Roman A, Daskalakis C, Ness A, Baxter JK. Gestational age at cervical length measurement and incidence of preterm birth. *Obstetrics Gynecol*. Aug; 2007 110(2 (Pt. 1)):311–317.
11. Lockwood CJ, Senyei AE, Dische MR, Casal D, Shah K, Thung S, Jones L, Deligdisgh L, Garite TJ. Fetal fibronectin in cervical and vaginal secretions as a predictor of preterm delivery. *New England J. Med*. 1991; 325(10):669–674. [PubMed: 1870640]
12. Honest H, Bachmann LM, Gupta JK, Kleijnen J, Khan KS. Accuracy of cervicovaginal fetal fibronectin test in. *Brit. Med. J*. 2002; 325(301):1–10. [PubMed: 12098707]
13. Foxman EF, Jarolim P. Use of the fetal fibronectin test in decisions to admit to hospital for preterm labor. *Clinical Chem*. Mar; 2004 50(3):661–663. [PubMed: 14981039]
14. Sanchez-Ramos L, Delke I, Zamora J, Kaunitz AM. Fetal fibronectin as a short-term predictor of preterm birth in symptomatic patients: A meta-analysis. *Obstetrics Gynecol*. Sep; 2009 114(3): 631–640.
15. Garfield RE, Saade G, Buhimschi C, Buhimschi I, Shi L, Shi S-Q, Chwalisz K. Control and assessment of the uterus and cervix during pregnancy and labour. *Human Reproduction Update*. 1998; 4(5):673–695. [PubMed: 10027621]
16. Garfield RE. Instrumentation for the diagnosis of term and preterm labour. *J. Perinat. Med*. 1998; 26:413–436. [PubMed: 10224598]
17. Mori Y, Ito A, Hirakawa K. The change in solubility of type I collagen in human uterine cervix in pregnancy at term. *Biochem. Med*. 1979; 21:262–270. [PubMed: 496919]
18. Kleissl HP, van der Rest M, Naftolin F, Glorieux FH, de Leon A. Collagen changes in the human uterine cervix at parturition. *Amer. J. Obstet. Gynecol*. 1978; 130(7):748–753. [PubMed: 637097]
19. Canty EG, Kadler KE. Procollagen trafficking, processing and fibrillogenesis. *J. Cell Sci*. Apr. 2005 118:1341–1353. [PubMed: 15788652]
20. Read CP, Word RA, Ruscheinsky MA, Timmons BC, Mahendroo MS. Cervical remodeling during pregnancy and parturition: Molecular characterization of the softening phase in mice. *Reproduction (Cambridge, England)*. Aug; 2007 134(2):327–340.
21. Drewes PG, Yanagisawa H, Starcher B, Hornstra I, Csiszar K, Marinis SI, Keller P, Word RA. Pelvic organ prolapse in fibulin-5 knockout mice: Pregnancy-induced changes in elastic fiber homeostasis in mouse vagina. *Amer. J. Pathol*. Feb; 2007 170(2):578–589. [PubMed: 17255326]
22. Ozasa H, Tominaga T, Nishimura T, Takeda T. Lysyl oxidase activity in the mouse uterine cervix is physiologically regulated by estrogen. *Endocrinology*. Aug; 1981 109(2):618–621. [PubMed: 6113953]
23. Granström L, Ekman G, Ulmsten U, Malmström A. Changes in the connective tissue of corpus and cervix uteri during ripening and labour in term pregnancy. *Brit. J. Obstetrics Gynaecol*. Oct; 1989 96(10):1198–1202.
24. Sokolov K, Galvan J, Myakov A, Lacy A, Lotan R, Richards-Kortum R. Realistic three-dimensional epithelial tissue phantoms for biomedical optics. *J. Biomed. Opt*. 2002; 7(1):148–156. [PubMed: 11818022]
25. Sennström MB, Ekman G, Westergren-Thorsson G, Malmström A, Byström B, Endréson U, Mlambo N, Norman M, Ståbi B, Brauner A. Human cervical ripening, an inflammatory process



- mediated by cytokines. *Molecular Human Reproduction*. Apr; 2000 6(4):375–381. [PubMed: 10729321]
26. Rath W, Osmer R, Adelmann-Grill BC, Stuhlsatz HW, Szevereny M, Kuhn W. Biochemical changes in human cervical connective tissue after intracervical application of prostaglandin E2. *Prostaglandins*. Apr; 1993 45(4):375–384. [PubMed: 8493359]
  27. Osmer R, Rath W, Pflanz MA, Kuhn W, Stuhlsatz HW, Szeverényi M. Glycosaminoglycans in cervical connective tissue during pregnancy and parturition. *Obstetrics Gynecol*. Jan; 1993 81(1): 88–92.
  28. Straach KJ, Shelton JM, Richardson JA, Hascall VC, Mahendroo MS. Regulation of hyaluronan expression during cervical ripening. *Glycobiology*. Jan; 2005 15(1):55–65. [PubMed: 15317739]
  29. El Maradny E, Kanayama N, Kobayashi H, Hossain B, Khatun S, Liping S, Kobayashi T, Terao T. The role of hyaluronic acid as a mediator and regulator of cervical ripening. *Human Reproduction (Oxford, England)*. May; 1997 12(5):1080–1088.
  30. Fraser JR, Laurent TC, Laurent UB. Hyaluronan: Its nature, distribution, functions and turnover. *J. Internal Med*. Jul; 1997 242(1):27–33. [PubMed: 9260563]
  31. Meyer K. The biological significance of hyaluronic acid and hyaluronidase. *Physiological Rev*. 1947; 27(3):335–359.
  32. Cunningham, FG.; Leveno, KJ.; Bloom, SL.; Hauth, JC.; Rouse, DJ.; Spong, CY. Parturition. In: Cunningham, FG.; Leveno, KJ.; Bloom, SL.; Hauth, JC.; Rouse, DJ.; Spong, CY., editors. *Williams Obstetrics*. 23rd ed.. McGraw-Hill; New York: 2010.
  33. Schlembach D, Mackay L, Shi L, Maner WL, Garfield RE, Holger M. Cervical ripening and insufficiency: From biochemical and molecular studies to in vivo clinical examination. *Eur. J. Obstetrics Gynecol. Reproductive Biol*. 2009; 144S:S70–S76.
  34. Maul H, Mackay L, Garfield RE. Cervical ripening: Biochemical, molecular, and clinical considerations. *Clinical Obstetrics Gynecol*. Sep; 2006 49(3):551–563.
  35. Garfield RE, Maner WL, Shi L, Shi SQ, Saade GR. Uterine EMG and cervical LIF—Promising technologies in obstetrics. *Current Women's Health Rev*. 2006; 2:207–221.
  36. Garfield RE, Maul H, Maner W, Fittkow C, Olson G, Shi L, Saade GR. Uterine EMG and light induced fluorescence in the management of term and preterm labor.pdf. *J. Soc. Gynecol. Investig*. 2002; 9:265–275.
  37. Grimnes, S.; Martinsen, OG. *Bioimpedance and Bioelectricity Basics*. 2nd ed.. Academic Press; Waltham, MA, USA: 2008.
  38. Avis NJ, Lindow SW, Kleinermann F. In vitro multifrequency electrical impedance measurements and modelling of the cervix in late pregnancy. *Physiological Meas*. Nov; 1996 17(Suppl. 4):A97–103.
  39. O'Connell MP, Tidy J, Wisher SJ, Avis NJ, Brown BH, Lindow SW. An in vivo comparative study of the pregnant and non-pregnant cervix using electrical impedance measurements. *BJOG: An Int. J. Obstetrics Gynaecol*. Aug; 2000 107(8):1040–1041.
  40. O'Connell MP, Avis NJ, Brown BH, Killick SR, Lindow SW. Electrical impedance measurements: An objective measure of prelabor cervical change. *J. Maternal-Fetal Neonatal Med.: Official J. Eur. Assoc. Perinatal Med., Fed. Asia Oceania Perinatal Societies, Int. Soc. Perinatal Obstetricians*. Dec; 2003 14(6):389–391.
  41. V Gandhi S, Walker DC, Brown BH, Anumba DOC. Comparison of human uterine cervical electrical impedance measurements derived using two tetrapolar probes of different sizes. *Biomed. Eng. Online*. 2006; 5:1–7.
  42. Jokhi RP, Brown BH, Anumba DOC. The role of cervical electrical impedance spectroscopy in the prediction of the course and outcome of induced labour. *BMC Pregnancy Childbirth*. Jan.2009 9:1–8. [PubMed: 19123930]
  43. Drezek R, Richards-kortum R. Understanding the contributions of NADH and collagen to cervical tissue fluorescence spectra: Modeling, measurements, and implications. *J. Biomed. Opt*. 2001; 6(4):385–396. [PubMed: 11728196]
  44. Rajan N, Habermehl J, Coté M-F, Doillon CJ, Mantovani D. Preparation of ready-to-use, storable and reconstituted type I collagen from rat tail tendon for tissue engineering applications. *Nature Protocols*. Jan; 2006 1(6):2753–2758. [PubMed: 17406532]

45. Oxlund BS, Ørtoft G, Brüel A, Danielsen CC, Bor P, Oxlund H, Ulbjerg N. Collagen concentration and biomechanical properties of samples from the lower uterine cervix in relation to age and parity in non-pregnant women. *Reproductive Biol. Endocrinol.: RB&E*. Jan.2010 8:1–9. [PubMed: 20051099]
46. Buckingham JC, Selden R, Danforth DN. Connective tissue changes in the cervix during pregnancy and labor. *Ann. N Y Acad. Sci.* 1962; 97:733–742. [PubMed: 14016554]
47. Norman M, Ekman G, Ulmsten U, Barchan K, Malmström A. Proteoglycan metabolism in the connective tissue of pregnant and non-pregnant human cervix. An in vitro study. *Biochemical J.* Apr; 1991 275(Pt 2):515–520.
48. Timmons B, Akins M, Mahendroo M. Cervical remodeling during pregnancy and parturition. *Trends Endocrinology Metabolism: TEM.* Jun; 2010 21(6):353–361.
49. Akins ML, Luby-Phelps K, Bank RA, Mahendroo M. Cervical softening during pregnancy: Regulated changes in collagen cross-linking and composition of matricellular proteins in the mouse. *Biol. Reproduction.* May; 2011 84(5):1053–1062.
50. Garfield RE, Maul H, Shi L, Maner W, Fittkow C, Olsen G, Saade GR. Methods and devices for the management of term and preterm labor. *Ann. New York Acad. Sci.* 2001; 943:203–224. [PubMed: 11594541]
51. Fittkow CT, Maul H, Olson G, Martin E, Mackay LB, Saade GR, Garfield RE. Light-induced fluorescence of the human cervix decreases after prostaglandin application for induction of labor at term. *Eur. J. Obstetrics Gynecol. Reproductive Biol.* 2005; 123:62–66.
52. Hoe YSG, Gurewitsch ED, Shaahinfar A, Hu ES, Sampattavanich S, Ruffner M, Ching KHS, Allen RH. Measuring bioimpedance in the human uterine cervix: Towards early detection of preterm labor. *Conf. Proc.: Annu. Int. Conf. IEEE Eng. Med. Biol. Soc.* Jan.2004 4:2368–2372.
53. Boehm D. The cervical cap: Effectiveness as a contraceptive. *J. Nurse-Midwifery.* 1983; 28(1):3–6. [PubMed: 6551434]
54. Gallo MF, Grimes DA, Schulz KF. Cervical cap versus diaphragm for contraception. *Cochrane Database Systematic Rev. (Online).* Jan.2002 (4):1–7.
55. Powell MG, Mears BJ, Deber RB, Ferguson D. Contraception with the cervical cap: Effectiveness, safety, continuity of use, and user satisfaction. *Contraception.* Mar; 1986 33(3):215–232. [PubMed: 3720304]
56. Garfield, RE.; Maner, WL. *Preterm. Birth*, Boca Raton. CRC Press; FL, USA: 2007. Biophysical methods of prediction and prevention of preterm labor: Uterine electromyography and cervical light-induced fluorescence—New obstetrical diagnostic techniques; p. 131-144.
57. Maul H, Saade G, Garfield RE. Prediction of term and preterm parturition and treatment monitoring by measurement of cervical cross-linked collagen using light-induced fluorescence. *Acta Obstet. Gynecol. Scand.* 2005; 84:534–536. [PubMed: 15901259]
58. Maul H, Olson G, Fittkow CT, Saade GR, Garfield RE. Cervical light-induced fluorescence in humans decreases throughout gestation and before delivery: Preliminary observations. *Amer. J. Obstetrics Gynecol.* Feb; 2003 188(2):537–541.
59. Glassman WS, Liao Q-P, Shi S-Q, Goodrum L, Olson G, Martin E, Saade G, Garfield RE. Fluorescence probe for cervical examination during various reproductive states. *Proc. SPIE—Adv. Fluorescence Sens. Technol. III.* 1997; 2980:286–292.
60. Eyre DR, Wu J-J. Collagen cross-links. *Top Curr. Chem.* 2005; 247:207–229.
61. Smith, JG. Ph.D. dissertation, School Phys. Chem. Sci. Queensland Univ. Technol.; Brisbane, Qld., Australia: 2008. Bioimpedance mapping of the cervix.
62. Filho, PB. Ph.D. dissertation. Dept. Med. Phys. Clinical Eng., University of Sheffield; South Yorkshire, U.K.: 2002. Tissue characterisation using an impedance spectroscopy probe.
63. Brown BH, Wilson AJ, Bertemes-Filho P. Bipolar and tetrapolar transfer impedance measurements from volume conductor. *Electron. Lett.* 2000; 36(25):2060–2062.
64. Grimnes S, Martinsen ØG. Sources of error in tetrapolar impedance measurements on biomaterials and other ionic conductors. *J. Phys. D: Appl. Phys.* Jan; 2007 40(1):9–14.
65. Gautieri A, Uzel S, Vesentini S, Redaelli A, Buehler MJ. Molecular and mesoscale mechanisms of osteogenesis imperfecta disease in collagen fibrils. *Biophysical J.* Aug; 2009 97(3):857–865.

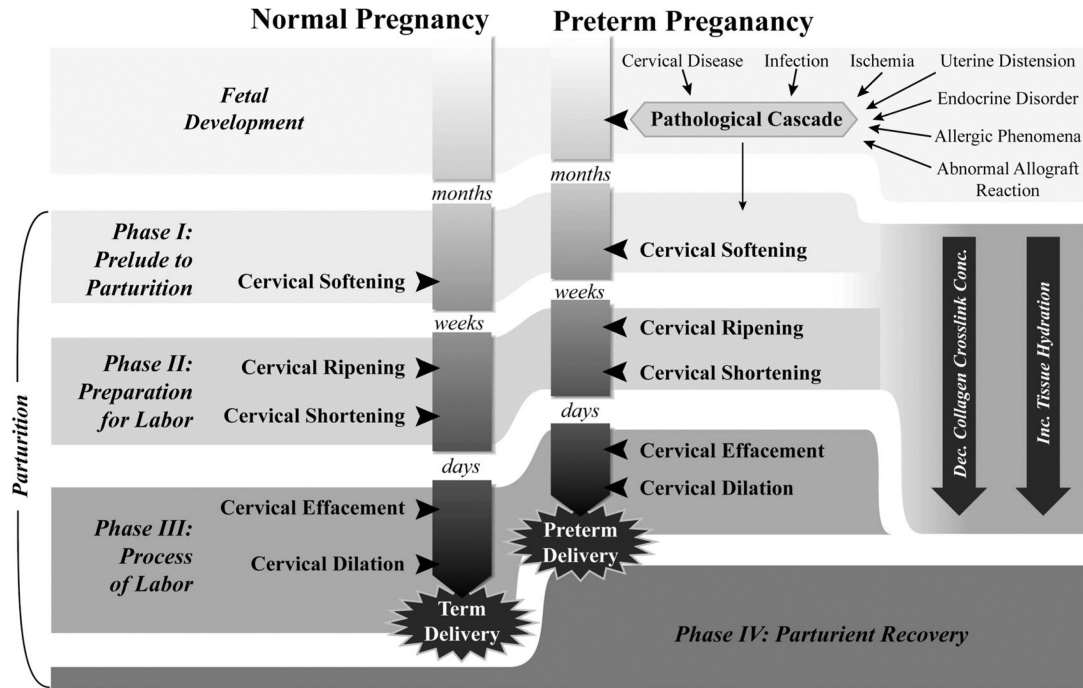


**Fig. 1.** All pregnancies must progress through the same clinical stages of parturition: cervical softening, ripening, shortening, effacement, dilation, and delivery. The currently held belief is that in preterm cases, various pathologies trigger pathological cascades long before preterm delivery occurs. These pathological cascades accelerate the parturition process with the ultimate outcome being premature labor and delivery. Current diagnostic techniques such as transvaginal ultrasound can only detect macroscopic changes in the parturition process such as cervical shortening. Clinicians currently do not have tools to objectively determine if and how quickly cervical softening and ripening are occurring. However, it is known that tissue microstructural reorganizations occur in cervical softening and ripening stages, notably a decrease in collagen crosslink concentration and an increase in tissue hydration. The ability to detect when these early parturition processes begin and the rate at which these processes progress may afford clinicians enough time to diagnose the underlying pathology to preterm birth, enabling new care models for managing preterm birth. Figure based on [4], [6], [32].

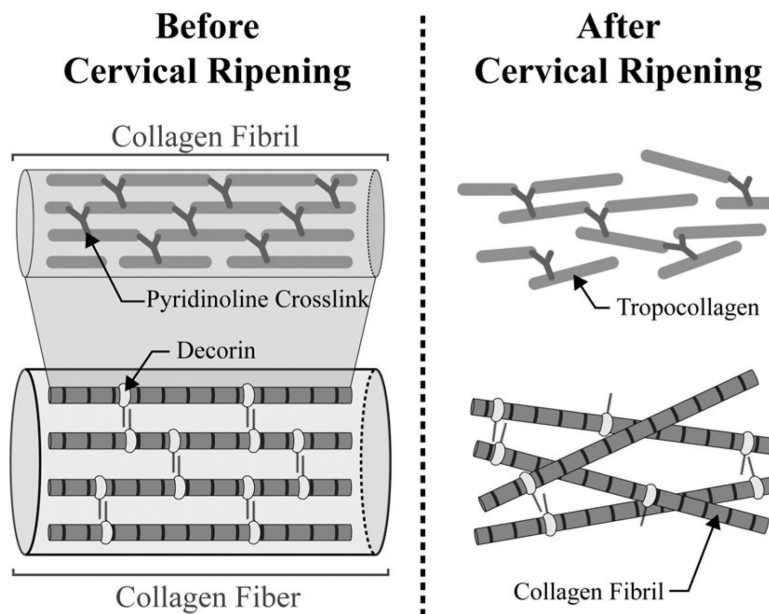


**Fig. 2.** Pyridinoline crosslinks are responsible for organizing tropocollagen helices into semicrystalline collagen fibrils. Each collagen fibril is then bundled into collagen fibers with proteoglycans such as decorin regulating packing density and arrangement. The cervical ripening process reduces both pyridinoline crosslinks and proteoglycan concentration, resulting in increased disorganization spanning two orders of structural arrangement. Figure based on [32], [60], [65].

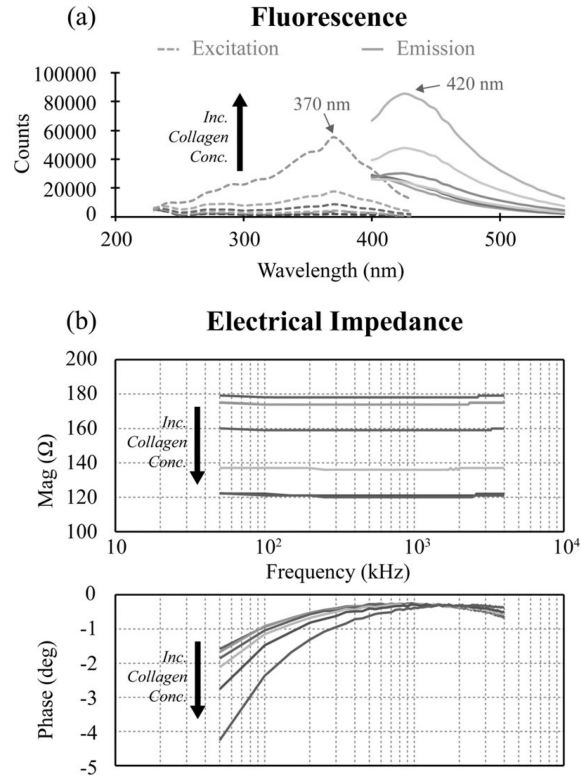


**Fig. 3.**

Collagen gels of concentrations 1, 2, 5, 10, 20, and 50 mg/mL were subjected to (a) bench top fluorescence spectroscopy, which shows the 370 nm excitation peak and the corresponding 420-nm emission peak characteristic of stromal collagen in the cervix. Increasing collagen concentration shows a proportional change in fluorescence counts. The same samples were also subjected to (b) bench top impedance spectroscopy from 55 kHz to 4 MHz. Results indicate that, for our collagen gel model, increases in collagen concentration are correlated with a decrease in impedance magnitude and phase. Collagen concentration-dependent differences in phase were greater at low and high frequencies. These data were used to inform *in vivo* circuit design parameters.

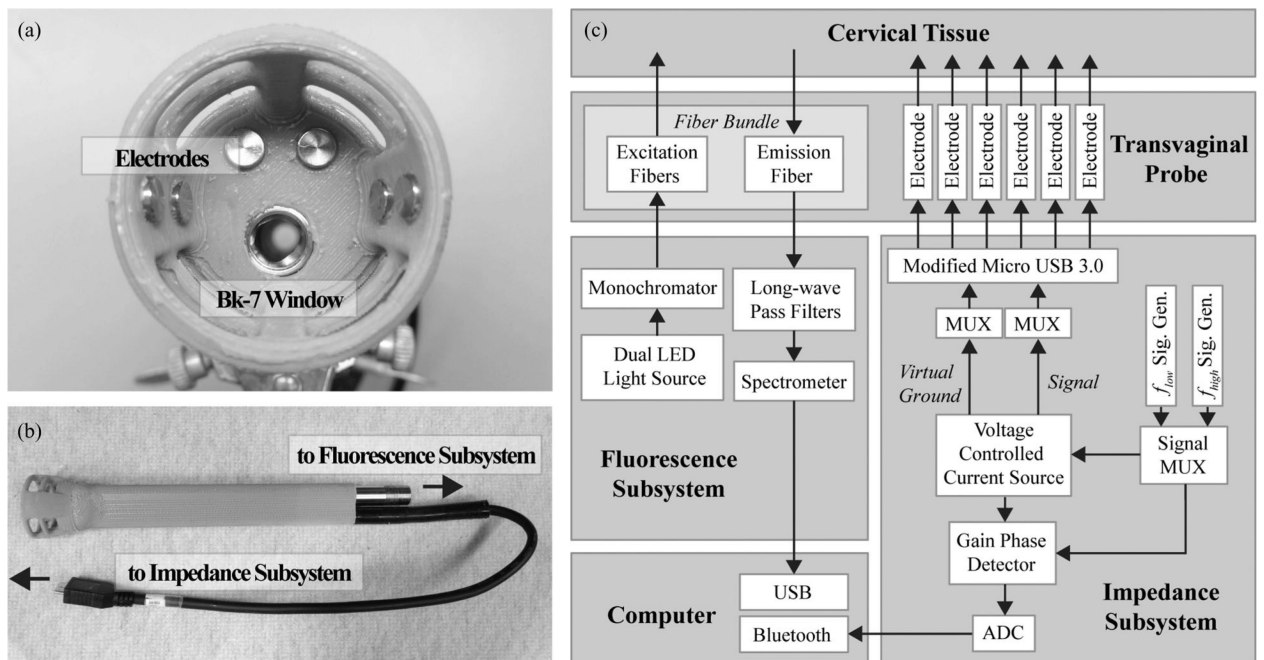


**Fig. 4.** (a) Head-on view of intravaginal probe showing the 6 electrodes and window for the fiber optic bundle. (b) Side view of intravaginal probe. (c) Block diagram depicting intravaginal probe, electrical impedance spectroscopy measurement subsystem, and light-induced fluorescence measurement subsystem.

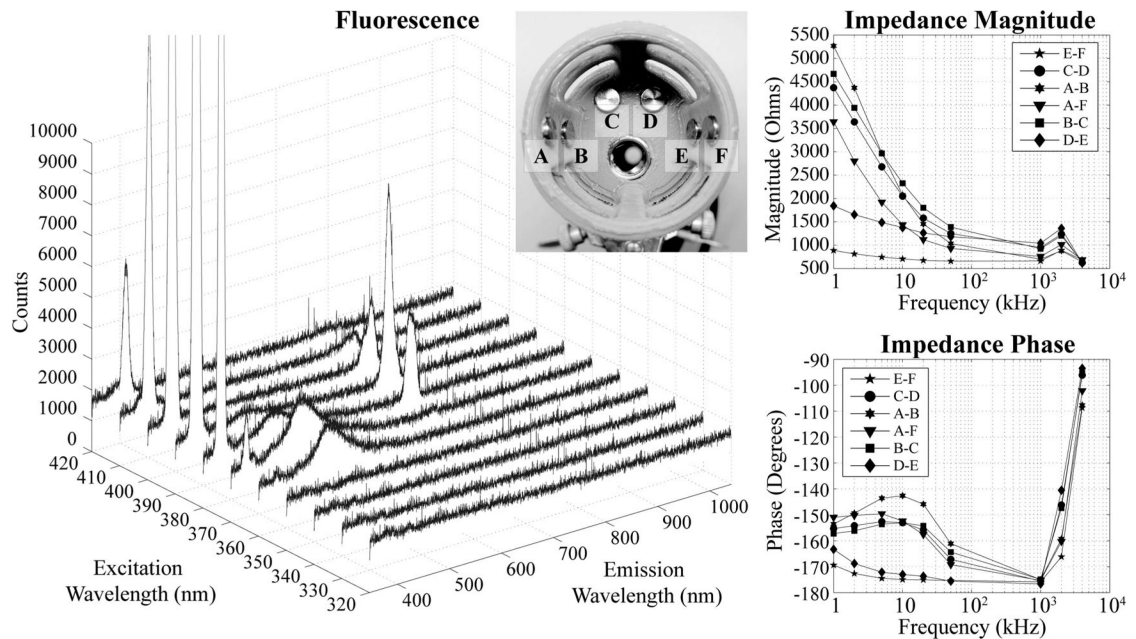


**Fig. 5.** Graphs depict a full scan measurement of raw LIF and EIS taken at the 12'o'clock position (BK7 window ventral) during week 37 of gestation. LIF measurements comprise of fluorescence emission spectra that result from an excitation scan from 320 to 420 nm at intervals of 10 nm. EIS measurements comprise of uncalibrated (see Section V-E) magnitude and phase measurements across pairs of electrodes that have different spatial orientations around the cervix.

**TABLE I**

Approximate Cost of Device Assembly for 30 Subjects

	Cost
Intravaginal Probe (30 Probes)	\$15,000
Impedance Subsystem	\$450
Fluorescence Subsystem	\$8,100
TOTAL	\$23,550
Per Subject Cost	\$785

Costs are approximate and include all material and manufacturing costs.

Author Manuscript

Author Manuscript

Author Manuscript

Author Manuscript